Supplementary Material for:

Catalytic Formation of Narrow Nb Nanowires Inside Carbon Nanotubes

Dan Liu, David Tománek*

Physics and Astronomy Department, Michigan State University, East Lansing, Michigan 48824, USA

1. Reaction pathway

As mentioned in the main manuscript, Nb is a refractory metal with a high melting temperature T_M = 2750 K that is close to the decomposition temperature of carbon nanotubes (CNTs). Thus, capillary filling, which had been used for other elements with a much lower melting point, including Pb, can not be used for Nb.

Formation of Pb nanowires by capillary filling is a relatively straight-forward process, as it only involves the condensation of Pb atoms within the void inside a nanotube,

$$\mathrm{Pb(g)} \longrightarrow \mathrm{Pb(s)}\ . \qquad \text{(S1)}$$

The reaction coordinate is the position of a single Pb atom in the 3-dimensional space and the reaction is thus easy to characterize.

For Nb, we propose a fundamentally different approach that yields metallic Nb as one of the products of a complex reaction that starts from the $NbCl_3$ molecular solid. As discussed in the main manuscript, this reaction is

$$10\mathrm{NbCl_3(s)} \longrightarrow 3\mathrm{Nb_2Cl_{10}(g)} + 4\mathrm{Nb(s)}\ . \qquad \text{(S2)}$$

With 40 atoms with 120 degrees of freedom involved, identifying the optimum reaction path in the 120-dimensional configuration space is practically impossible. Understanding this reaction is a serious challenge in Inorganic Chemistry.

We have attempted to run molecular dynamics simulations reflecting the reaction Eq. (S2) under high-pressure and high-temperature conditions to get guidance regarding the likely reaction path, but failed due to the limited simulation time. We have concluded that

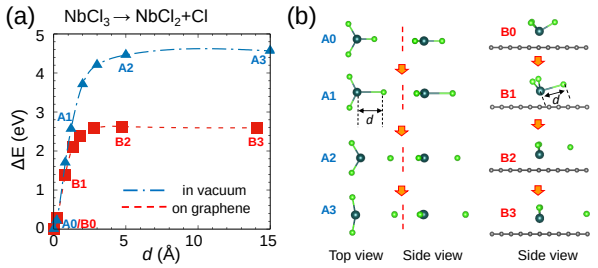

Figure S1: Dissociation of $NbCl_3$ to $NbCl_2$ and Cl according to Eq. (S3) in vacuum and on graphitic carbon. (a) Energetics of the reaction in vacuum (data points A0–A3, connected by the blue dash-dotted line) and on graphitic carbon (data points B0–B3, connected by the red dashed line). (b) Snap shots of the intermediate geometries. The reaction coordinate is represented by d, the length of one particular Nb-Cl bond.

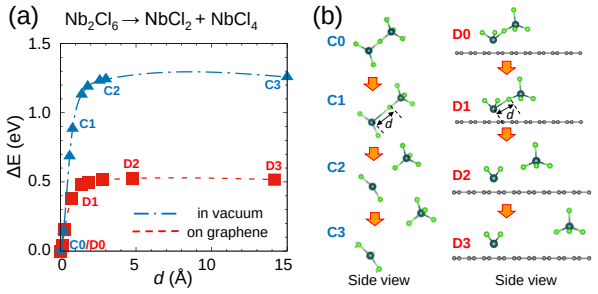

Figure S2: Transformation of Nb_2Cl_6 to $NbCl_2$ and $NbCl_4$ according to Eq. (S4) in vacuum and on graphitic carbon. (a) Energetics of the reaction in vacuum (data points C0–C3, connected by the blue dash-dotted line) and on graphitic carbon (data points D0–D3, connected by the red dashed line). (b) Snap shots of the intermediate geometries. The reaction coordinate is represented by d, the length of one particular Nb-Cl bond.

locating intermediate structures and transition states for a reaction as complex as in Eq. (S2) is not feasible computationally.

Still, we can provide results of limited calculations for processes that likely take place during the complex reaction in Eq. (S2), both in vacuum and inside a carbon

*Corresponding author
Email address: tomanek@pa.msu.edu (David Tománek)

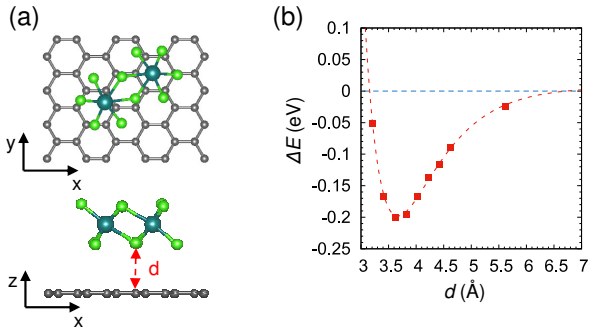

Figure S3: Interaction of an Nb_2Cl_{10} molecule with a graphene monolayer.(a) Side and top views of the molecule at the distance d from graphene. (b) Interaction energy $\Delta E(d)$ between an Nb_2Cl_{10} molecule and graphene.

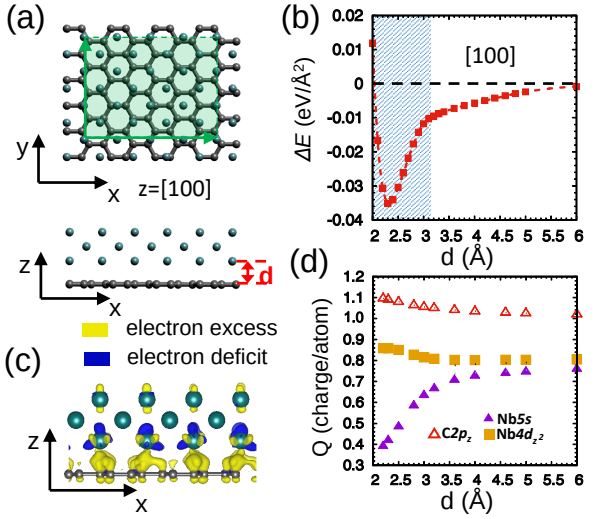

Figure S4: Interaction of the Nb(100) surface with a graphene monolayer. (a) Top and side views of the atomic arrangement, with the supercell highlighted by red. (b) Interaction energy ΔE between the Nb(100) surface and graphene as a function of the separation distance d. (c) Charge redistribution caused by the interaction of Nb(100) with graphene, superposed with the atomic structure. $\Delta\rho$ = ρ(Nb/graphene)−ρ(Nb)−ρ(graphene) is shown by isosurfaces bounding regions of electron excess at $+4\times10^{-3}$ e/Å^3 (yellow) and electron deficiency at -4×10^{-3} e/Å^3 (blue). (d) Mulliken charge of specific atomic orbitals as a function of d.

nanotube.

One reaction step that is likely to occur in this complex reaction is the detachment of a chlorine atom from an $NbCl_3$ molecule of the starting substance according to

$$NbCl_3(g) \longrightarrow NbCl_2(g) + Cl(g)\ . \qquad \text{(S3)}$$

The energetics of the corresponding endothermic dissociation process, which may occur in vacuum or on

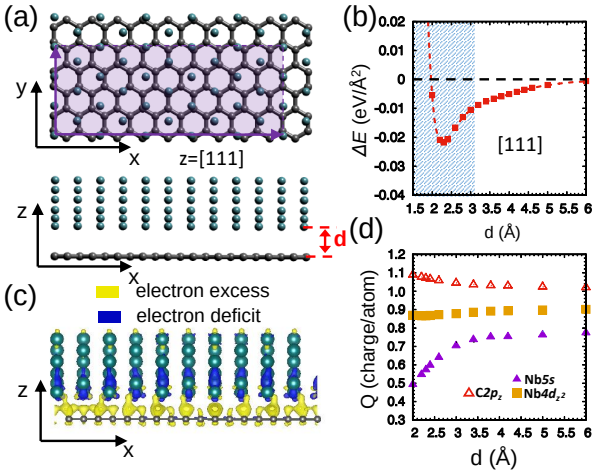

Figure S5: Interaction of the Nb(111) surface with a graphene monolayer. (a) Top and side views of the atomic arrangement, with the supercell highlighted by red. (b) Interaction energy ΔE between the Nb(111) surface and graphene as a function of the separation distance d. (c) Charge redistribution caused by the interaction of Nb(111) with graphene, superposed with the atomic structure. $\Delta\rho$ = ρ(Nb/graphene)−ρ(Nb)−ρ(graphene) is shown by isosurfaces bounding regions of electron excess at $+4\times10^{-3}$ e/Å^3 (yellow) and electron deficiency at -4×10^{-3} e/Å^3 (blue). (d) Mulliken charge of specific atomic orbitals as a function of d.

graphitic carbon, is presented in Fig. S1 along with the corresponding geometries. Clearly, the dissociation energy is lowered significantly in presence of graphitic carbon.

Another reaction likely to occur during the conversion of $NbCl_3$ to metallic Nb and other molecules is the dimerization of $NbCl_3$ to Nb_2Cl_6, followed by simultaneous detachment of a Cl atom from $NbCl_3$ while a new Nb-Cl bond is being formed with another $NbCl_3$ molecule. One reaction that reflects simultaneous dissociation and formation of an Nb-Cl bond is

$$Nb_2Cl_6(g) \longrightarrow NbCl_2(g) + NbCl_4(g)\ . \qquad \text{(S4)}$$

The energetics of this endothermic dissociation process, which may occur in vacuum or on graphitic carbon, is illustrated in Fig. S2 along with the corresponding geometries.. Clearly, the energy barrier is lowered in presence of graphitic carbon also for this reaction.

2. Interaction of $NbCl_5$ with graphene

$NbCl_5$ dimerizes to Nb_2Cl_{10} molecules shown in Figure S3(a). In contrast to $NbCl_3$ discussed in the main manuscript, there is only one shallow 'physisorption' state of Nb_2Cl_{10} on graphene, as seen in Figure S3(b). The physisorption energy $\Delta E = -0.2$ eV is

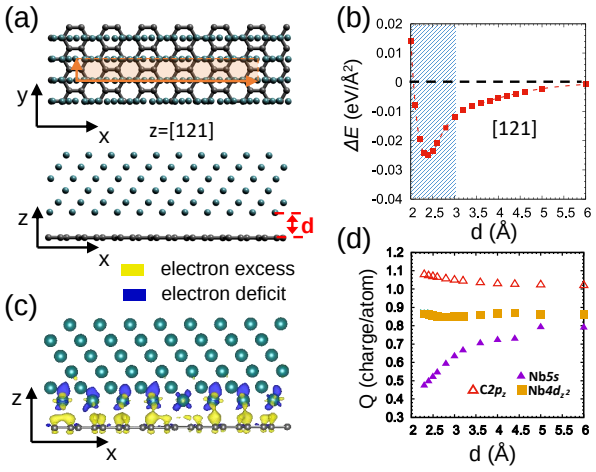

Figure S6: Interaction of the Nb(121) surface with a graphene monolayer. (a) Top and side views of the atomic arrangement, with the supercell highlighted by red. (b) Interaction energy ΔE between the Nb(121) surface and graphene as a function of the separation distance d. (c) Charge redistribution caused by the interaction of Nb(121) with graphene, superposed with the atomic structure. $\Delta\rho = \rho$(Nb/graphene)$-\rho$(Nb)$-\rho$(graphene) is shown by isosurfaces bounding regions of electron excess at $+4\times10^{-3}$ e/Å^3 (yellow) and electron deficiency at -4×10^{-3} e/Å^3 (blue). (d) Mulliken charge of specific atomic orbitals as a function of d.

very small and the charge transfer between the molecule and graphene is negligible.

3. Interaction of Nb(100), Nb(111) and Nb(121) surfaces with graphene

An analogy to the results for interaction of Nb(110) with graphene, presented in Figure 3 of the main manuscript, we present results for graphene interacting with Nb(100) in Figure S4, Nb(111) in Figure S5, and Nb(121) in Figure S6.

4. Electronic structure of bulk $NbCl_5$

We have optimized the bulk structure of two bulk allotropes of $NbCl_5$ using density functional theory (DFT) as specified in the main manuscript. We have found their energies to differ by *lesssim*1 meV per formula unit, indicating that the two allotropes are equally stable. We present the DFT-based electronic density of states (DOS) in Fig. S7. In view of the fact the DFT eigenvalues always underestimate the fundamental band gap, both allotropes are clearly wide-gap semiconductors.

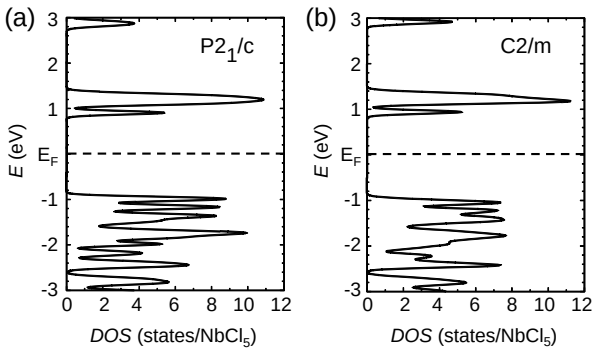

Figure S7: Electronic density of states (DOS) of two monoclinic bulk allotropes of niobium pentachloride. (a) $NbCl_5$ with $P2_1/c$ symmetry and 24 atoms in total per unit cell. (b) $NbCl_5$ with $C2/m$ symmetry and 72 atoms in total per unit cell. Both crystals are wide-gap semiconductors.